

# Very massive underground detectors for proton decay searches<sup>1</sup>

A. Rubbia

Institut für Teilchenphysik, ETHZ, CH-8093 Zürich, Switzerland

## Abstract

Massive underground detectors can be considered as sort of observatories for rare physics phenomena like astrophysical neutrino detection and nucleon decay searches. We briefly overview the past tracking calorimeters developed for nucleon decay searches. We then discuss the two technologies which are discussed today for potential future applications: Water Cerenkov ring imaging (WC) and liquid Argon Time Projection Chamber (LAr TPC). We present a conceptual design for a 100 kton liquid Argon TPC. We illustrate the physics performance of Water Cerenkov and liquid Argon TPC detectors for the  $p \rightarrow e^+\pi^0$  and  $p \rightarrow \nu K^+$  proton decay searches. We briefly compare the physics reach of the two techniques. We conclude by stressing the complementarity of the two approaches, noting however that, given the foreseeable timescale for these next generation experiments, the new challenging technique of the LAr TPC might offer more discovery potentials.

## 1 Introduction

### 1.1 The physics of massive underground detectors

Most massive underground detectors were designed by optimizing their performance for the search of nucleon decays. In this short review, we will discuss these detectors under this point of view, however, massive underground detectors have a much larger physics program, for example with the observation and study of astrophysical (solar, atmospheric, and supernova neutrinos) and artificial beam neutrinos. Such a comprehensive physics program, possibly with non-accelerator and accelerator-based components, makes massive underground detectors “general purpose” facilities, sort of observatories for rare physics phenomena.

Nucleon decay studies are presently in a “second generation” phase, after the enthusiasm following the development of the first GUT theories. The minimal version of SU(5)[1], predicting the decay  $p \rightarrow e^+\pi^0$  with a lifetime of about  $10^{31}$  years, has been ruled out by the experimental limits ( $\tau > 2.9 \times 10^{33}$  years), and also fails to predict the correct value of  $\sin^2 \theta_W$ . Alternative models have been proposed, for instance SUSY GUTs, that predict values of  $\sin^2 \theta_W$  closer to the measured ones, and the presence of an intermediate mass scale of  $O(M_W)$ , that seems to provide a better unification of the coupling constants, at higher values with respect to minimal SU(5)[2]. The higher unification mass pushes up the proton lifetime in the  $p \rightarrow e^+\pi^0$  channel, which has predicted lifetimes of  $10^{36\pm 1}$  years, compatible with the experimental limits. However, in this scenario, other decay channels open up,

<sup>1</sup>Based on an invited talk at the XI International Conference on Calorimetry in High Energy Physics - CALOR2004, Perugia, Italy, March 2004.

where supersymmetric intermediate states are involved. In particular, s-quark production is favoured, and final states involving kaons (like  $p \rightarrow K^+\nu$ ) are present.

## 1.2 Detector optimization

Nucleon decay signals are characterized by (a) their topology (b) their kinematics. By topology, we mean the necessary presence of a lepton (an electron, a muon or a neutrino) in the final state, in general, few particles in the end products (for example, two body decays are believed to be favored), and obviously no other energetic nucleon in the final state. The exact kinematics of the event depends on the type of target. For free protons (target with hydrogen), the total momentum of the event should be compatible with zero, while for nucleon decays occurring in nuclear targets, we expect a smearing from Fermi motion and also other nuclear effects (rescattering, absorption, etc.). The total energy of the event should be equal to the nucleon mass, which means in the GeV range.

As far as detector optimizations are concerned, we stress three points needed to reach stringent sensitivities on nucleon lifetime with low backgrounds: (1) the necessity of fine tracking (2) the necessity of excellent resolution (3) the necessity of large masses. We discuss these points in the following.

The fine tracking (hence high spatial resolution) is a fundamental tool for the visualization of the event and for the particle identification. This is of extreme importance to separate potential signal from background. Discovery experiments should by definition be low background, in order to make possible claims based on few events. Ideally, one would like to have 3 dimensional tracking and vertex reconstruction. For particle identification, stopping power measurement ( $dE/dx$ ) is important to separate low momentum particles. Integration of  $dE/dx$  yields the kinetic energy. The separation of electrons, muons, protons, pions and kaons in the momentum ranges between  $\simeq 10$  and  $\simeq 100$  MeV/c is wanted. Good particle identification is specially required for  $\mu/\pi$  and  $e/\pi^0$  separation.

Table 1: Massive underground experiments for nucleon decay searches

Detector	Date	Type	Location	Typ. mass
NUSEX	1982	Tracking calorimeter	Mont-Blanc, France	0.15 kton
Fréjus	1985	Tracking calorimeter	Fréjus, France	0.9 kton
Soudan	1989	Tracking calorimeter	Minnesota, USA	0.96 kton
Kamiokande	1983	Water Cerenkov	Gifu, Japan	0.88 kton
IMB-3	1986	Water Cerenkov	Ohio, Japan	3.3 kton
Super-Kamiokande	1996	Water Cerenkov	Gifu, Japan	22.5 kton
ICARUS	2006(?)	Liquid Argon	Gran Sasso, Italy	0.6→ 3 kton

Precise calorimetric information in the GeV region requires high sampling rate and containment of the particles and showers (e,  $\pi^0$ , ...). The shower direction is also needed for kinematical reconstruction. Calorimetric performance has an impact on the granularity of the detector.

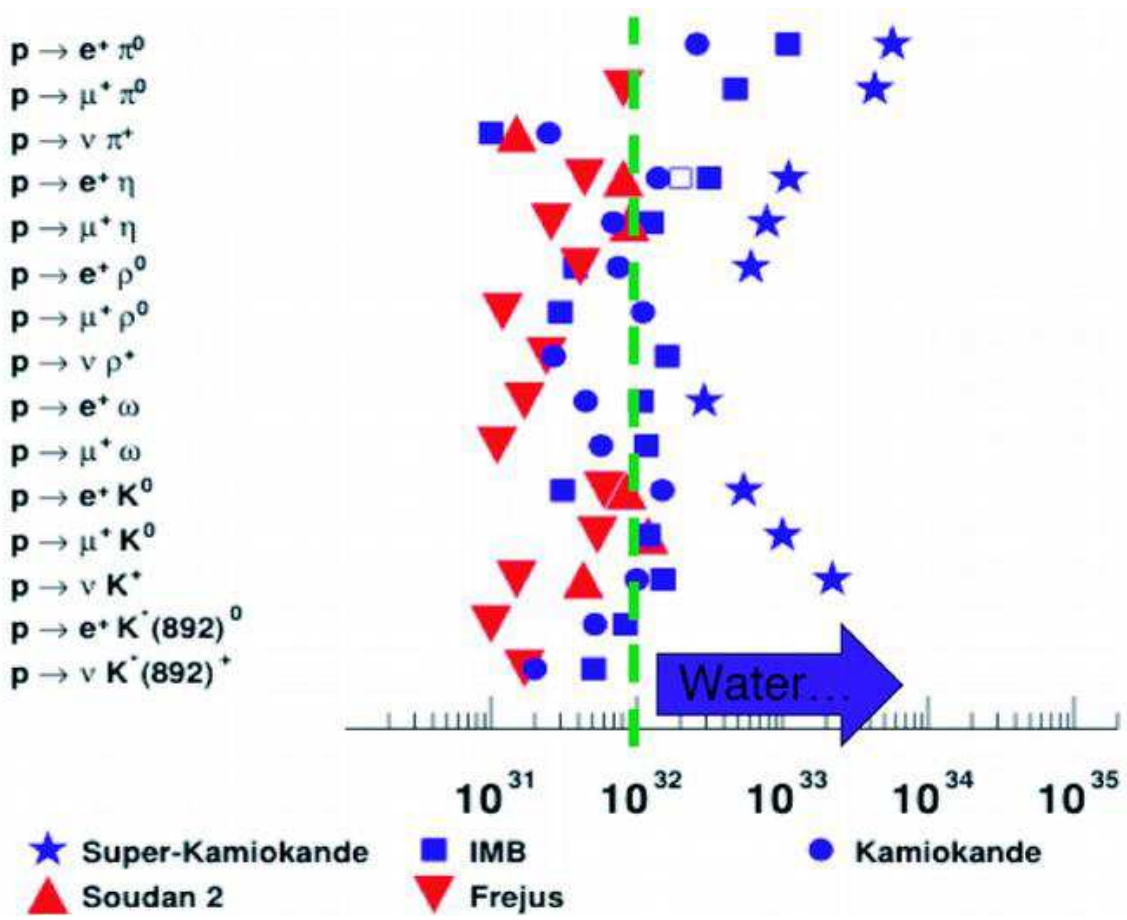


Figure 1: Illustration of current experimental limits on nucleon lifetime.

Finally, the mass scale of the detectors is given by the nucleon lifetime scale. Since there is about  $6 \times 10^{32}$  nucleons per kton of mass, the proton lifetime limit in case of no backgrounds (and no signal!) is simply given by:

$$\tau_p/Br (90\%C.L.) > 10^{32} \text{years} \times M(\text{kton}) \times T(\text{yr}) \times \epsilon \quad (1)$$

where  $M$  is the detector mass in kton,  $T$  is the exposure in years and  $\epsilon$  is the signal detection efficiency after cuts, which depends on the considered decay channel. If background (mainly coming from atmospheric neutrinos when the detector is located deep underground) is present, the sensitivity increases only proportionally to  $\sqrt{M}$ .

Given the variety of predicted decay modes, the ideal detectors should be as versatile as possible, very good in background rejection, and at the same time have the largest possible mass. The relevant factor is in fact  $Mass \times \epsilon$ , hence, large masses must be coupled to fine tracking and excellent calorimetry, to suppress backgrounds with a good signal detector efficiency.

## 2 Nucleon decay experiments

A list of massive underground experiments for nucleon decay searches is given in Table 1. Their typical masses are given in the last column of the table. We note that NUSEX, Fréjus, Soudan, Kamiokande and IMB stopped data-taking and currently only Superkamiokande is active. ICARUS is under construction and is the only planned new experiment. Other bigger detectors are being discussed with timescales likely beyond the year 2015 and will be mentioned later.

A summary of the current limits on nucleon decays is illustrated in Figure 1. We note a clear separation line at the level of  $\simeq 10^{32}$  years. Above this value, Water Cerenkov (in fact, Superkamiokande) results dominate. This shows that the factor for improving “limits” in nucleon decay has been mass. The fine granularity calorimeter, which provided a priori a better information on events, did not yield limits beyond  $\simeq 10^{32}$  years because of their limited mass. The best limits are currently in the range of  $\simeq 10^{33}$  years. As will be shown later, improving sensitivities beyond the currently achieved results will require very large masses but also good detector performances. Indeed, the Water Cerenkov technique is reaching the level at which background events start to become reducible only at the cost of signal efficiency. In this regime, the gain in sensitivity will not be linear with mass anymore. We will show that the liquid Argon TPC technique provides better performance than Water Cerenkov detectors and can therefore solve the problem of backgrounds, so the question is how large a liquid Argon TPC can be? Before we discuss this point, we summarize in the following sections (1) the basic features of the tracking calorimeters and (2) the Water Cerenkov detectors and their performance for two proton decay channels.

## 3 Tracking calorimeters

### 3.1 NUSEX experiment

NUSEX[3] was composed of iron plates interleaved with streamer tubes. Its average density was  $3.5 \text{ g/cm}^3$ . The total mass was 150 tons. In total there were 134 horizontal iron plates, each plate has dimensions of  $3.5 \text{ m} \times 3.5 \text{ m} \times 1 \text{ cm}$ . The streamer tubes were made of plastic ( $3.5 \text{ m}$  long,  $9 \times 9 \text{ mm}^2$  cross-section) with digital readout. The tracking was provided by the planes of tubes equipped with X & Y pickup strips for two dimensional localization. The total number of tubes was 42880. The gas mixture was  $Ar - CO_2(15\%) - npentane(1+2+1)$ . The resolution was  $0.3 \text{ cm}$  in the X-view,  $0.37 \text{ cm}$  in Y and the track separation was about  $1.5 \text{ cm}$ . A test module was exposed to electrons at the CERN PS with momenta ranging from  $0.150$  to  $2 \text{ GeV}/c$  at varying angles ( $0 \rightarrow 40^\circ$ ). The energy resolution was  $\sigma/E \approx 0.13/\sqrt{E(\text{GeV})} \oplus 0.2$ . Muons and pions momentum was estimated with range. Poor separation between them was possible. One particularity was the exposure of a test module to actual neutrinos at CERN. A beam of  $10 \text{ GeV}$  protons was sent on a Be target which was configured in a beam-dump mode. The decay length was  $10 \text{ m}$  and was followed by  $12 \text{ m}$  of Fe/concrete shielding. The detector was exposed at two angles and the following statistics was collected: 210 (0 deg) and 184 (45 deg) neutrino interactions were identified. These were used directly to estimate the background in nucleon decay searches. The nucleon decay results of NUSEX can be found in Ref.[4]. It is interesting to note the existence of a candidate in the  $p \rightarrow \mu^+ K^0$  mode which had an estimated background of 0.09.

## 3.2 Fréjus experiment

The Fréjus experiment[5] was a modular tracking calorimeter composed of 912 layers of sandwich of 3 mm thick iron and  $5 \times 5 \text{ mm}^2$  plastic flash tubes coupled with  $15 \times 15 \text{ mm}^2$  Geiger tubes for triggering. The total mass was 900 tons and the average density  $1.95 \text{ g/cm}^3$ . The detector dimensions were 6 m (wide)  $\times$  12.3 m (deep)  $\times$  6 m (high). The absorber was iron. The readout was done via the 6 m long flash tubes whose discharge was triggered by a signal in the corresponding Geiger tubes. The flash tubes contained a Neon(70%)-Helium(30%) mixture and were pulsed with 5 kV for a duration  $> 800 \text{ ns}$  with a fast rise-time ( $< 100 \text{ ns}$ ) not to act as a clearing field. The long time was needed to propagate the discharge down the 6 m long tubes. The tracking was obtained by the orientation of the planes in various directions. In total, there were  $10^6$  tubes. The spatial resolution was about 5 mm. The electromagnetic resolution was  $\sigma/E \approx 0.06/\sqrt{E(\text{GeV})} \oplus 0.055$ . A pizero mass distribution was reconstructed and had a width of 16%. Muons and pions momentum was estimated with range. Poor separation between them was possible. Results on nucleon decay can be found in Ref.[6]. The relatively good tracking performance of the system can be appreciated in the list of final states searched by the Fréjus experiment.

## 3.3 Soudan experiment

The Soudan-II experiment[7] was characterized as a fine grain, finely segmented calorimeter. The detector was composed of 224 calorimeter modules for a total mass of 960 tons. Each module had a mass of 4.3 tons and a volume of 1 m (wide)  $\times$  1.11 m (deep)  $\times$  2.7 m (high). The absorber was composed of corrugated iron sheets yielding an average density of  $1.6 \text{ g/cm}^3$ . The readout was made possible by 1 m long drift tubes with a diameter of 1.5 cm. Tracking was provided by the tubes readout which allowed for three spatial coordinates and  $dE/dx$  measurement. The total number of tubes was  $\approx 2 \times 10^6$ . The maximum drift in the tubes was 50 cm and the gas mixture was  $Ar - CO_2(15\%)$  yielding a drift velocity of  $0.6 \text{ cm}/\mu\text{s}$  at 180 V/cm. The resolutions were 0.38 cm in the xy-plane and 0.65 cm in the z-direction. Nucleon decay results from the Soudan-II experiment can be found in Ref.[8].

# 4 Water Cerenkov detectors

## 4.1 The technique

This technique was developed in the first large scale detectors Kamiokande[9] and IMB[10]. The largest detector existing today is the Superkamiokande[11] Water Cerenkov detector. It is composed of a tank of 50 kton of water (22.5 kton fiducial) which is surrounded by 11146 20-inch phototubes immersed in the water. About 170  $\gamma/\text{cm}$  are produced by relativistic particles in water in the visible wavelength  $350 < \lambda < 500 \text{ nm}$ . With 40% PMT coverage and a quantum efficiency of 20%, this yields  $\approx 14$  photoelectrons per cm or  $\approx 7$  p.e. per MeV deposited. Contrary to the fine tracking calorimeters described in the previous section, water provides free protons in 20% of the cases, which should yield events without Fermi smearing. The performance of the Superkamiokande detector is good, regardless of its coarse imaging nature. The vertex resolution is about 30 cm for 1-ring events and estimated to be 15 cm for  $p \rightarrow e^+ \pi^0$  events. The trigger threshold is set at 5 MeV photoelectron equivalent, which means the triggering of nucleon decay is 100% efficient. The energy resolution is

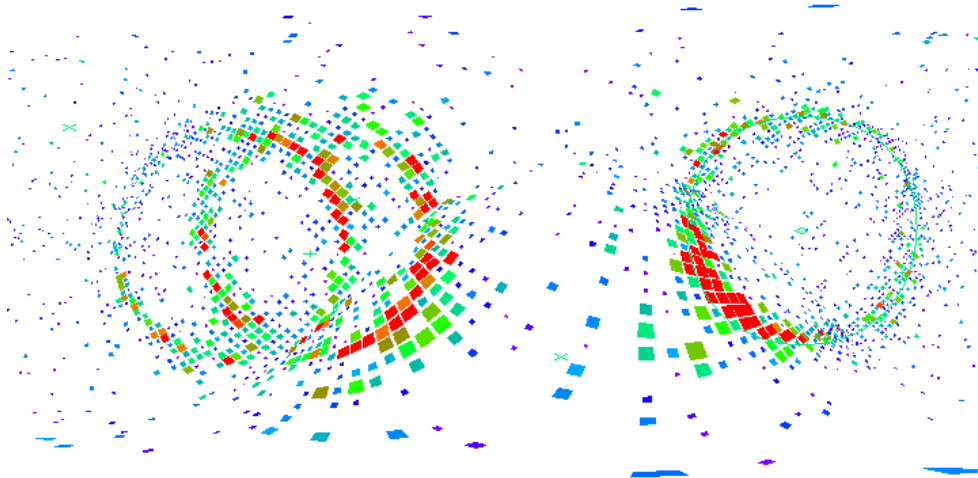


Figure 2: MC event of  $p \rightarrow e^+\pi^0$  in Superkamiokande[30].

approximately 3–4% for electrons and muons. Strikingly enough particle identification is made possible by the features of the Cerenkov rings: fuzzyness signals electrons while sharp-edged rings indicate muons. The particle separation is better than 99% for muons and electrons. In case of  $p \rightarrow e^+\pi^0$  and  $p \rightarrow \mu^+\pi^0$  it is greater than 97%. One major drawback is the high Cerenkov momentum threshold, namely 568 MeV/c for kaons and 1070 MeV/c for protons! This implies for example that kaons produced in  $p \rightarrow K^+\nu$  are invisible.

## 4.2 Results on proton decay

In Water Cerenkov detectors, an ideal  $p \rightarrow e^+\pi^0$  event might look like Figure 2. This event was generated with a detailed  $p \rightarrow e^+\pi^0$  event and detector Monte Carlo (MC) simulation[30]. In this figure, the PMTs are plotted as a function of  $\cos\theta$  vs.  $\phi$  as viewed from the event vertex and are represented by squares, colored by amount of collected charge (red is more, blue is less) and sized to show distance from the event vertex. The fuzzy outer edges of the rings indicate an electromagnetic showering type of ring.

Superkamiokande searches for the  $p \rightarrow e^+\pi^0$  mode with selection criteria that are as follows[30] (See Table 2): (A)  $6000 < Q_{tot} < 9500$  photoelectrons (PEs), (B) 2 or 3 e-like (showering type) rings, (C) if 3 rings:  $85 < M_{inv,\pi^0} < 185$  MeV/c<sup>2</sup>, (D) no decay electrons, (E)  $800$  MeV/c<sup>2</sup>  $< M_{inv,tot} < 1050$  MeV/c<sup>2</sup>, and (F)  $P_{tot} = \left| \sum \vec{P}_i \right| < 250$  MeV/c. The criterion (A) corresponds to a loose energy cut which reduces the background without much computation needed. As stated above, it is possible for one of the photons to be invisible, for which (B) allows. If there are 3 rings criterion (C) requires that 2 of the rings reconstruct to give a  $\pi^0$  mass. Since there are no muons nor charged pions expected, no decay electrons should be found and any events which have them will be cut by (D). Finally (E) requires the total invariant mass to be near that of the proton and (F) requires the total reconstructed momentum (magnitude of the vector sum of all individual momenta) to be below the Fermi momentum for <sup>16</sup>O. Figure 3 shows distributions of  $p \rightarrow e^+\pi^0$  MC, atmospheric MC, and data in reconstructed momentum vs. invariant mass after criteria (A)-(D) have been applied. Criteria (E) and (F) are shown by the box.

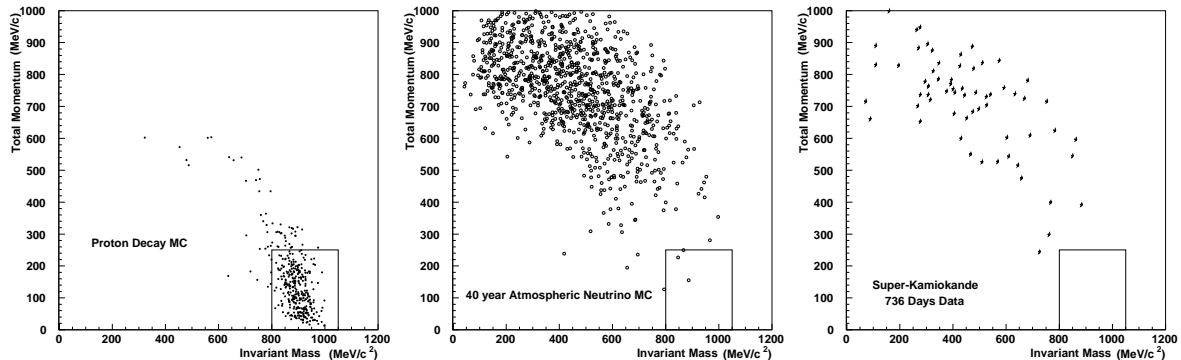


Figure 3:  $p \rightarrow e^+\pi^0$  mode. Distributions of events in total reconstructed momentum *vs.* total invariant mass for (a) proton decay MC, (b) atmospheric neutrino MC, and (c) data.

When these criteria are applied to 45 kton-years (736 days) of data Superkamiokande finds no candidate events. Using atmospheric neutrino background MC equivalent to 40 years of data taking it is estimated that 0.2 background events are expected in the data. From MC simulations of  $p \rightarrow e^+\pi^0$  events, the efficiency to select any  $p \rightarrow e^+\pi^0$  events in the data sample is 44%. This gives a limit on the proton lifetime divided by  $p \rightarrow e^+\pi^0$  branching ratio (partial limit) of  $\tau/B_{p \rightarrow e^+\pi^0} > 2.9 \times 10^{33}$  years (90% CL).

Table 2: Water: Analysis for the  $p \rightarrow e^+\pi^0$  channel[30].

	$p \rightarrow e^+\pi^0$	MC	Data
6000 < $Q_{tot}$ < 9500 p.e.			
2 or 3 e-like rings			
85 < $M_{inv,\gamma\gamma}$ < 185 MeV (if 3 rings)			
no decay electron			
800 < $M_{inv}$ < 1050 MeV			
$\sum p < 0.250$ GeV	44%	0.2	0

Superkamiokande searches for the  $p \rightarrow \bar{\nu}K^+$  mode[30] by looking for the products from the two primary branches of the  $K^+$  decay:  $K^+ \rightarrow \mu^+\nu_\mu$  and  $K^+ \rightarrow \pi^+\pi^0$ . In the  $K^+ \rightarrow \mu^+\nu_\mu$  case, when the decaying proton is in the  $^{16}\text{O}$ , the nucleus will be left as an excited  $^{15}\text{N}$ . Upon de-excitation, a prompt 6.3 MeV photon will be emitted. So this second branch has two independent searches: one in which the signature of this prompt photon is required and one in which it is explicitly absent.

When searching for the  $p \rightarrow \bar{\nu}K^+$ ;  $K^+ \rightarrow \mu^+\nu_\mu$  with a 6.3 MeV prompt photon search the following criteria are required: (A) 1  $\mu$ -like ring, (B) 1 decay electron, (C)  $215 < P_\mu < 260$  MeV/c, and (D)  $N_{PMT} > 7$ ;  $12 < t_{PMT} < 120$  ns before  $\mu$  signal. The only particle giving a visible ring is the mono-energetic muon. Criteria (A-C) select for that. In criterion (D),  $t_{PMT}$  is the time a PMT was hit subtracted by the time it would take a photon to get directly from the fit event vertex to the PMT (so called “time minus time of flight” or “timing residual”).

This search has an efficiency of 4.4%, finds no candidates on an estimated background of 0.4 events, and sets a limit of  $\tau/B_{p \rightarrow \bar{\nu}K^+; (\gamma)K^+ \rightarrow (\gamma)\mu^+\nu_\mu} > 2.1 \times 10^{32}$  years (90% CL).

The complementary case where no prompt gamma is allowed has the same criteria as the prompt gamma case except for the last: (D)  $N_{PMT} \leq 7$ ;  $12 < t_{PMT} < 120$  ns before  $\mu$

signal. Since this allows a significant amount of background to survive the selection criteria, the limit is set by fitting for an excess of proton decay events above the atmospheric neutrino background in the reconstructed momentum spectrum. In this region, 70 candidate events are found which is consistent with the 74.5 events expected from atmospheric neutrinos. With an efficiency of 40% a limit of  $\tau/B_{p \rightarrow \bar{\nu}K^+; (\gamma)K^+ \rightarrow (\gamma)\mu^+\nu_\mu} > 3.3 \times 10^{32}$  years (90% CL) is found.

The criteria for the  $p \rightarrow \bar{\nu}K^+; K^+ \rightarrow \pi^+\pi^0$  search are as follows: (A) 2 e-like rings, (B) 1 decay electron, (C)  $85 < M_{inv,\pi^0} < 185$  MeV/c<sup>2</sup>, (D)  $175 < P_{\pi^0} < 250$  MeV/c, (E)  $40 < Q_{\pi^+} < 100$  PE. The  $\pi^+$  is very close to Cerenkov threshold and is expected to only produce a small amount of light as in (E). Since this is not enough to produce an identifiable ring only the rings from the 2 photons from the decay of the  $\pi^0$  are required in (A). These photons must reconstruct to an invariant mass in the range defined by (C) as well as a momentum range defined in (D). No candidates are found and 0.7 background events are expected. The selection efficiency is 6.5%, giving a partial lifetime limit of  $\tau/B_{p \rightarrow \bar{\nu}K^+; K^+ \rightarrow \pi^+\pi^0} > 3.1 \times 10^{32}$  years (90% CL).

The combined limit for these three topologies is  $\tau/B_{p \rightarrow \bar{\nu}K^+; K^+ \rightarrow \mu^+\nu_\mu} > 6.8 \times 10^{32}$  years (90% CL).

### 4.3 Future plans

Given the large existing experience in large underground Water Cerenkov detectors, a certain number of conceptual ideas have been put forward in order to increase further the mass by at least an order of magnitude compared to the largest Superkamiokande detector. These are summarized in the last column of Table 3. The size of these detectors will eventually be limited by the light attenuation in water, however, this length is measured to be in the range of 100 m in Superkamiokande. Hence, the limiting factor is rather driven by the size of the underground cavern and by the cost of the experiment. A way to reduce costs is to limit the effective photocathode coverage however at the cost of physics performance. To set the scale, Superkamiokande has a design coverage of 40%. A one-megaton HyperK[31] with similar performance would contain between 100'000–200'000 large area (8 inch) photomultipliers.

Table 3: Comparison of Water Cerenkov Detectors

Parameters	Kamioka Japan	IMB-3 USA	SuperK Japan	SNO Canada	HyperK[31] (proposed)	UNO[32] (proposed)	3M[33] (proposed)
Mass kt	4.5	8	50	8	1000	650	1000
Fiducial	1.0	3.3	22	2	800	440	800
Effective							
Photocathode coverage	20%	4%	40%	60%	20–40%	1/3 10% 2/3 40%	14%



## 5 Large Liquid Argon imaging TPC

### 5.1 The technique

Among the many ideas developed around the use of liquid noble gases, the Liquid Argon Time Projection Chamber (LAr TPC), conceived and proposed at CERN by C. Rubbia in 1977 [13], certainly represented one of the most challenging and appealing designs. The technology was proposed as a tool for uniform and high accuracy imaging of massive detector volumes. The operating principle of the LAr TPC was based on the fact that in highly purified LAr ionization tracks could indeed be transported undistorted by a uniform electric field over distances of the order of meters [14]. Imaging is provided by wire planes placed at the end of the drift path, continuously sensing and recording the signals induced by the drifting electrons. Liquid Argon is an ideal medium since it provides high density, excellent properties (ionization, scintillation yields) and is intrinsically safe and cheap, and readily available anywhere as a standard by-product of the liquefaction of air.

The feasibility of this technology has been further demonstrated by the extensive ICARUS R&D program, which included studies on small LAr volumes about proof of principle, LAr purification methods, readout schemes and electronics, as well as studies with several prototypes of increasing mass on purification technology, collection of physics events, pattern recognition, long duration tests and readout. The largest of these devices had a mass of 3 tons of LAr [15, 16] and has been continuously operated for more than four years, collecting a large sample of cosmic-ray and gamma-source events. Furthermore, a smaller device with 50 l of LAr [17] was exposed to the CERN neutrino beam, demonstrating the high recognition capability of the technique for neutrino interaction events.

The realization of the 600 ton ICARUS detector culminated with its full test carried out at surface during the summer 2001 [18]. This test demonstrated that the LAr TPC technique can be operated at the kton scale with a drift length of 1.5 m. Data taking of about 30000 cosmic-ray triggers have allowed to test the detector performance in a quantitative way and results have been published in [19, 20, 21, 22, 23].

### 5.2 A conceptual design for a 100 kton detector

A conceptual design for a 100 kton LAr TPC was given in Ref. [24]. The basic design features of the detector can be summarized as follows: (1) Single 100 kton “boiling” cryogenic tanker at atmospheric pressure for a stable and safe equilibrium condition (temperature is constant while Argon is boiling). The evaporation rate is small (less than  $10^{-3}$  of the total volume per day given by the very favorable area to volume ratio) and is compensated by corresponding refilling of the evaporated Argon volume. (2) Charge imaging, scintillation and Cerenkov light readout for a complete (redundant) event reconstruction. This represents a clear advantage over large mass, alternative detectors operating with only one of these readout modes. The physics benefit of the complementary charge, scintillation and Cerenkov readout are being assessed. (3) Charge amplification to allow for very long drift paths. The detector is running in bi-phase mode. In order to allow for drift lengths as long as  $\sim 20$  m, which provides an economical way to increase the volume of the detector with a constant number of channels, charge attenuation will occur along the drift due to attachment to the remnant impurities present in the LAr. This effect can be compensated with charge amplification near the anodes located in the gas phase. (4) Absence of magnetic field,

although this possibility might be considered at a later stage. Physics studies [25] indicate that a magnetic field is really only necessary when the detector is coupled to a Neutrino Factory.

The cryogenic features of the proposed design are based on the industrial know-how in the storage of liquefied natural gases (LNG,  $T \simeq 110$  K at 1 bar), which developed quite dramatically in the last decades, driven by the petrochemical and space rocket industries. LNG are used when volume is an issue, in particular, for storage. The technical problems associated to the design of large cryogenic tankers, their construction and safe operation have already been addressed and engineering problems have been solved by the petrochemical industry. The current state-of-the-art contemplates cryogenic tankers of 200000 m<sup>3</sup> and their number in the world is estimated to be  $\sim 2000$  with volumes larger than 30000 m<sup>3</sup> with the vast majority built during the last 40 years. Technodyne International Limited, UK [26], which has expertise in the design of LNG tankers, has been appointed to initiate a feasibility study in order to understand and clarify the issues related to the operation of a large underground LAr detector. A final report is expected soon.

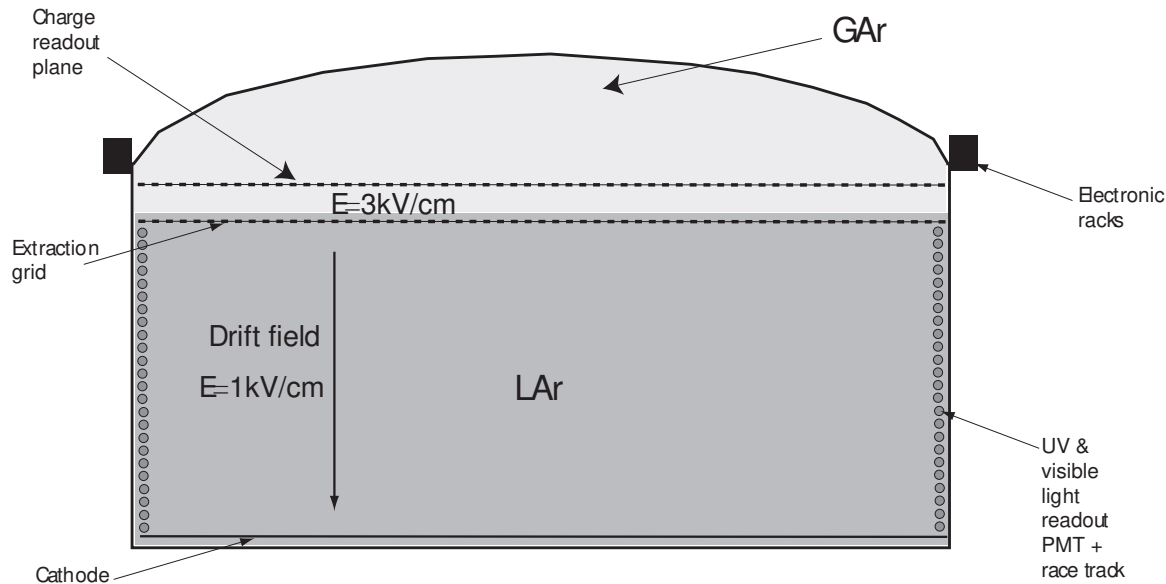


Figure 4: Schematic layout of a 100 kton liquid Argon detector. The race track is composed of a set of field shaping electrodes.

A schematic layout of the inner detector is shown in Figure 4. The detector is characterized by the large fiducial volume of LAr included in a large tanker, with external dimensions of approximately 40 m in height and 70 m in diameter. A cathode located at the bottom of the inner tanker volume creates a drift electric field of the order of 1 kV/cm over a distance of about 20 m. In this field configuration ionization electrons are moving upwards while ions are going downward. The electric field is delimited on the sides of the tanker by a series of ring electrodes (race-tracks) placed at the appropriate potential by a voltage divider.

The tanker contains both liquid and gas Argon phases at equilibrium. Since purity is a concern for very long drifts of 20 m, we assume that the inner detector could be operated in bi-phase mode: drift electrons produced in the liquid phase are extracted from the liquid into the gas phase with the help of a suitable electric field and then amplified near the anodes. In order to amplify the extracted charge one can consider various options: amplification near

thin readout wires, GEM [27] or LEM [28]. Studies that we are presently conducting show that gain factors of 100-1000 are achievable in pure Argon [29]. Amplification operates in proportional mode. Since the readout is limited to the top of the detector, it is practical to route cables out from the top of the dewar where electronics crates can be located around the dewar outer edges.

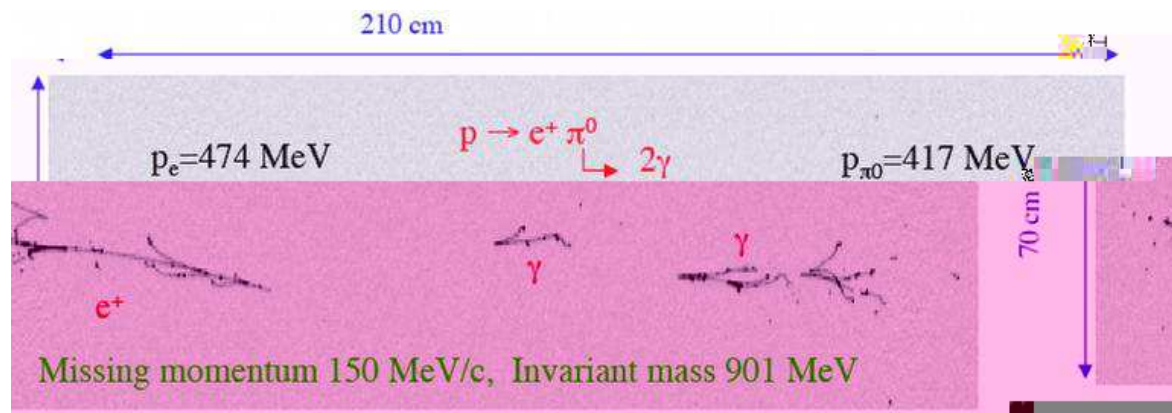


Figure 5: MC event of  $p \rightarrow e^+ \pi^0$  in a liquid Argon TPC.

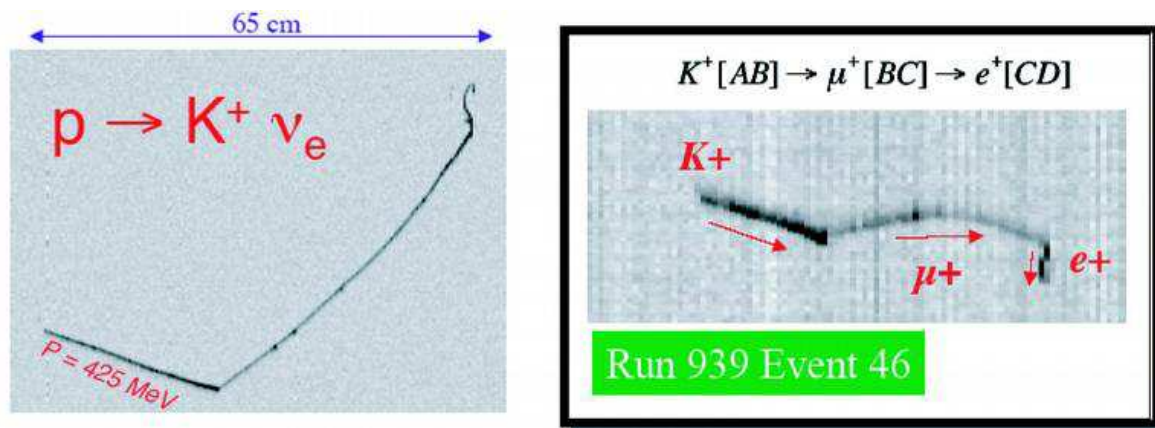


Figure 6: (left) MC event of  $p \rightarrow K^+ \nu$  in a liquid Argon TPC. (right) Real event collected in ICARUS T600 cosmic run performed on surface with a stopping kaon topology

After a drift of 20 m at 1 kV/cm, the electron cloud diffusion reaches approximately a size of 3 mm, which corresponds to the envisaged readout pitch. Therefore, 20 m practically corresponds to the longest conceivable drift path. As mentioned above, drifting over such distances will be possible allowing for some charge attenuation due to attachment to impurities. If one assumes that the operating electron lifetime is at least  $\tau \simeq 2$  ms (this is the value obtained in ICARUS T600 detector during the technical run [22] and better values of up to 10 ms were reached on smaller prototypes during longer runs), one then expects an attenuation of a factor  $\sim 150$  over the distance of 20 m. This loss will be compensated by the proportional gain at the anodes. We remind that the expected attenuation factor (compensated by the amplification) will not introduce any detection inefficiency, given the value of  $\sim 6000$  ionization electrons per millimeter produced along a minimum ionizing track in LAr.

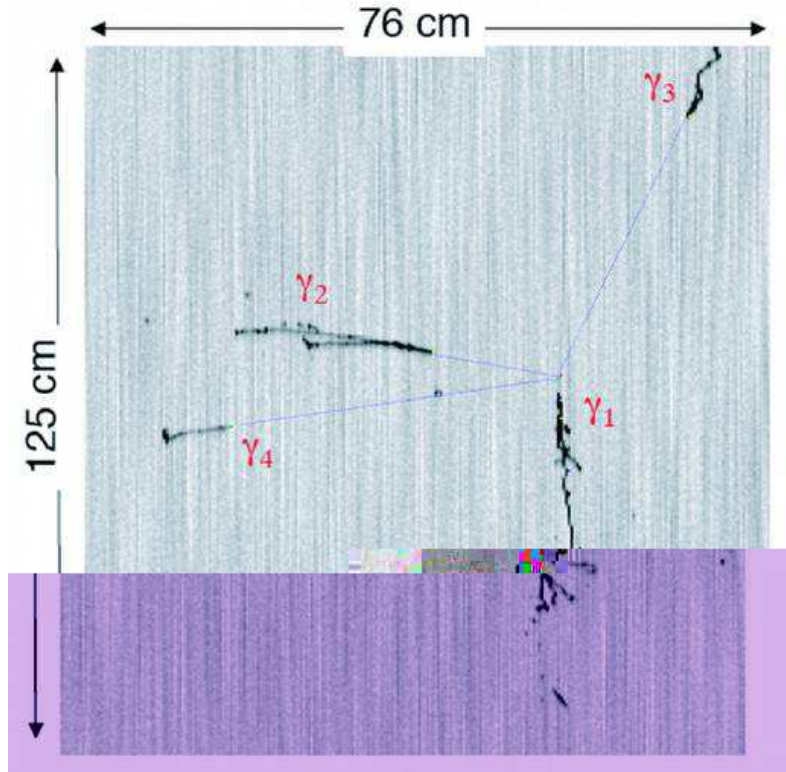


Figure 7: MC event of  $n \rightarrow \nu K^0 \rightarrow \nu \pi^0 \pi^0$  in a liquid Argon TPC.

In addition to charge readout, one can envision to locate PMTs around the inner surface of the tank. Scintillation and Cerenkov light can be readout essentially independently. LAr is a very good scintillator with about 50000  $\gamma/\text{MeV}$  (at zero electric field). However, this light is essentially distributed around a line at  $\lambda = 128 \text{ nm}$  and, therefore, a PMT wavelength shifter (WLS) coating is required. Cerenkov light from penetrating muon tracks has been successfully detected in a LAr TPC [21]; this much weaker radiation (about 700  $\gamma/\text{MeV}$  between 160 nm and 600 nm for an ultrarelativistic muon) can be separately identified with PMTs without WLS coating, since their efficiency for the DUV light will be very small.

A series of R&D is ongoing to further develop the conceptual ideas outlined above and are discussed in Ref.[34].

### 5.3 Estimated sensitivities to nucleon decay searches

In absence of data, the sensitivity to nucleon decay has been studied carefully with MC simulations, which include all known physics and detector effects. Overall the searches largely profit, regardless of the decay mode, of the clear imaging properties which allows to unambiguously tag most events. In particular, low particle detection thresholds are very effective at suppressing atmospheric neutrino events. Examples of signal events are shown in Figures 5, 6 and 7. In Figure 6 we included a real event collected in a ICARUS T600 cosmic run performed on surface. The real event shows very well the topology of the kaon, muon decay chain. In particular, the figure shows the power of multiple  $dE/dx$  measurements.

For the  $p \rightarrow e^+ \pi^0$  channel, one finds that the  $\pi^0$  is absorbed via nuclear interaction about

45% of the times. This is comparable to what happens on Oxygen, as the probability for interaction scales with  $A^{1/3}$ , hence, the ratio of rate of interaction between Oxygen and Argon is  $(A_O/A_{Ar})^{(1/3)} \approx 0.77$ .

A list of cuts is presented in Table 4. Rates are normalized to an exposure of 1000 kton $\times$ year. The signal events are required to be balanced (up to Fermi motion), with all particles identified as such and with a total invariant mass compatible with that of a proton. After the requirement for one  $\pi^0$  and one positron (or electron), only  $\nu_e$  and  $\bar{\nu}_e$  CC events survive. It should be stressed that the study of the background did not at this stage rely on a full simulation and reconstruction of events hence has to be considered as preliminary. Work is in progress to better estimate reconstruction effects. Finally a cut on reconstruction momentum and energy is sufficient to reject all backgrounds, leaving less than 1  $\nu_e$  CC event. The signal efficiency is 45%.

Table 4: Liquid Argon: Cuts for the  $p \rightarrow e^+ \pi^0$  channel. Survival fraction of signal (first column) and background events through event selections applied in succession.

	$p \rightarrow e^+ \pi^0$	$\nu_e$ CC	$\bar{\nu}_e$ CC	$\nu_\mu$ CC	$\bar{\nu}_\mu$ CC	$\nu$ NC	$\bar{\nu}$ NC
	100%	59861	11707	106884	27273	64705	29612
One $\pi^0$	54.0%	6604	2135	15259	5794	8095	3103
One positron	54.0%	6572	2125	20	0	0	0
No charged pions	53.9%	3605	847	5	0	0	0
No protons	50.9%	1188	656	1	0	0	0
$\sum p < 0.4$ GeV	46.7%	454	127	0	0	0	0
$0.86 < E < 0.95$ GeV	45.3%	< 1	0	0	0	0	0

The  $p \rightarrow \nu K^+$  channel profits from the expected excellent kaon identification capability. The probability that the kaon interacts inside the nuclear matter is also very small since strangeness should be conserved. A list of cuts is presented in Table 5, normalized to an exposure of 1000 kton $\times$ year. At this level of sophistication in the analysis, it appears that positive particle identification and a single kinematical cut on the total energy is sufficient to totally reduce all backgrounds keeping an efficiency of 97% for the signal. This efficiency is about an order of magnitude larger than that obtained in Water Cerenkov detectors, as illustrated in previous sections. Work is in progress to further understand these figures, in particular concerning strange production backgrounds due to cosmic ray muons as a function of the underground depth[35].

Table 5: Liquid Argon: Cuts for the  $p \rightarrow K^+ \bar{\nu}$  channel. Survival fraction of signal (first column) and background events through event selections applied in succession.

Cuts	$p \rightarrow K^+ \bar{\nu}$	$\nu_e$ CC	$\bar{\nu}_e$ CC	$\nu_\mu$ CC	$\bar{\nu}_\mu$ CC	$\nu$ NC	$\bar{\nu}$ NC
	100%	59861	11707	106884	27273	64705	29612
One Kaon	96.75%	308	36	871	146	282	77
No $\pi^0$	96.75%	143	14	404	56	138	25
No positrons	96.75%	0	0	400	56	138	25
No muons	96.75%	0	0	0	0	138	25
No charged pions	96.75%	0	0	0	0	57	9
Total Energy < 0.8 GeV	96.75%	0	0	0	0	< 1	0

## 6 Large Water Cerenkov or Liquid Argon TPC ? or both?

### 6.1 One versus the other?

Among all the technologies considered today, the Water Cerenkov and the liquid Argon TPC are the only ones that have the highest potential to provide a rich physics program, including both accelerator and non-accelerator aspects. Therefore, it is a relevant question to ask which detector should be adopted for the next generation massive underground detector on the timescale of the next decade. On one hand, the liquid Argon TPC is a superior imaging technology than the Water technology. On the other hand, the experience in massive underground Water Cerenkov detector is much greater than in the case of the liquid Argon TPC.

Indeed, the Water Cerenkov technology, is a very robust, proven and well-understood technology. It was demonstrated to the 50 kton scale with Superkamiokande, which was operated underground for many years. A megaton-scale detector, like the HyperKamiokande one, is perceived as a “straight-forward” extrapolation of Superkamiokande. Provided that a megaton-scale detector is financeable, the question that needs to be understood is whether a twenty-fold increase in statistics compared to Superkamiokande will answer the important physics questions of the next decade.

On the other hand, the liquid Argon TPC is a new and challenging technology. It is the fruit of many years of R&D effort conducted by the ICARUS collaboration. It was demonstrated up to the 0.6 kton scale on the surface test in summer 2001. An extrapolation from 0.6 to 100 kton is certainly a big step. A conceptual design based on the well-proven LNG technology was proposed and is being elaborated. Nonetheless, extrapolation to 100 kton might require an intermediate step, a 10% prototype ( $\simeq 10$  kton), to prove that the LNG technology and the physics can be fruitfully married in an actual experiment. In addition to the mass increase, the imaging provided by such a detector would provide a qualitative and quantitative improvement in the physics program. R&D efforts are on-going and must be vigorously pursued. In parallel, high statistics, precision physics will require a  $\simeq 100$  ton detector acting as a near experiment in a neutrino beam. This step is mandatory in order to improve the knowledge of neutrino interactions on Argon and the ability to reconstruct them with a liquid Argon TPC.

### 6.2 Both – complementarity

In an ideal configuration, an optimum physics program would exploit the complementarity between the two techniques in order to best answer the physics questions. We illustrate this complementarity in the case of the proton decay searches in Figure 8, where the sensitivity to  $p \rightarrow e^+\pi^0$  and  $p \rightarrow \nu K^+$  are plotted as a function of the exposure for the two techniques (WC and LAr). In this plot, the contribution of the background has been included. This explains the see-saw behavior of the sensitivities as soon as backgrounds are greater than 1 event. In this case, we always assumed that the actually observed number of events is identical to the expected (to the nearest integer of course). The two graphs show that: (1) for  $p \rightarrow e^+\pi^0$  the larger exposure of WC is important; (2) for the  $p \rightarrow \nu K$  mode, the imaging of LAr largely compensates for the reduced mass. This kind of argument can be extended to other decay modes, by realizing that WC detectors are most sensitive to electromagnetic and

back-to-back configurations, but are rather limited in tracking performance, in detection of heavy or slow charged particles, and in multi-particle final-states.

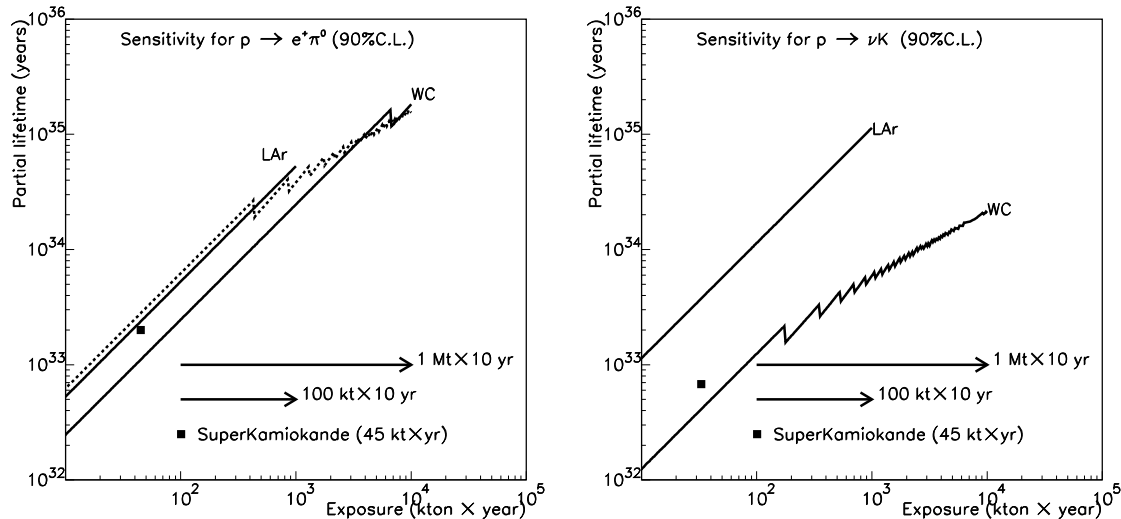


Figure 8: Expected sensitivity of Water Cerenkov (WC) and liquid Argon TPC (LAr) detectors for  $p \rightarrow e^+\pi^0$  and  $p \rightarrow \nu K$  decays. For WC, we assumed similar performance as in SuperK. The dashed line for the  $p \rightarrow e^+\pi^0$  channel corresponds to the standard SK cut, while the thick line corresponds to the “tight” cut analysis.

Table 6 summarizes these features in a more quantitative way. We also list in the Table relevant figures for other non-accelerator physics topics, like the observation of supernova explosions (SN), and solar and atmospheric neutrinos. Once again the complementarity between the two techniques, assuming a 650 kton water Cerenkov and a 100 kton liquid Argon TPC, is visible.

## 7 Conclusion

Massive tracking calorimeters were developed as ideal tools to look for nucleon decays and for a wide underground physics program. The increase in mass of the fine grain tracking calorimeters (NUSEX, Fréjus and SOUDAN) became quickly limited. The main scaling problem of these technologies is that channel count (and therefore cost) scale with the mass of the detector, since they instrument the volume. Hence, detectors in the tens of kton range with high granularity are impractical.

Water Cerenkov (WC) detectors do not possess the fine granularity of the “tracking calorimeters”, however, can be built in very large sizes since the instrumentation scales with the surface of the detector and not the volume. WC detectors provided very stringent *limits* on nucleon decays, thanks to their mass scales. Given their coarse imaging, their sensitivity is limited to mostly electromagnetic back-to-back nucleon decay events and given the background levels in many channels, their sensitivity is expected to scale with the square root of their mass and exposure. The era of the linear sensitivity gain with mass is over for various channels.

Table 6: Comparison of Water Cerenkov and Liquid Argon TPC detector

	Water Cerenkov (UNO)	Liquid Argon TPC
Total mass	650 kton	100 kton
$p \rightarrow e\pi^0$ in 10 yrs	$1.6 \times 10^{35}$ yrs ( $\epsilon \approx 17\%$ , $\approx 1$ evts background)	$0.5 \times 10^{35}$ yrs ( $\epsilon \approx 45\%$ , $\approx 1$ evt background)
$p \rightarrow \nu K$ in 10 yrs	$0.2 \times 10^{35}$ yrs ( $\epsilon \approx 8.6\%$ , $\approx 57$ evts background)	$1.1 \times 10^{35}$ yrs ( $\epsilon \approx 97\%$ , $\approx 1$ evt background)
$p \rightarrow \mu\pi K$ in 10 yrs	N/A	$8 \times 10^{34}$ yrs ( $\epsilon \approx 98\%$ , $\approx 1$ evt background)
SN cool off 10 kpc	194000 (mostly $\bar{\nu}_e p \rightarrow e^+ n$ )	38500 (all flavors) (64000 if nh-L mixing)
SN in Andromeda	40 events	7 (12 if nh-L mixing)
SN burst 10 kpc	$\approx 330$ $\nu - e$ elastic scattering	380 $\nu_e$ CC (flavor sensitive)
SN relic	Yes	Yes
Atmospheric neutrinos	60000 events/yr	10000 events/yr
Solar neutrinos	$E_e > 7MeV$ (central module)	324000 events/yr with $E_e > 5MeV$

In the meantime, the liquid Argon imaging TPC has reached a high level of maturity thanks to the extensive R&D conducted by the ICARUS Collaboration during many years. Today, quantitative progress in nucleon decay is calling for an application of this technology at the 100 kton mass scale. We have shown a new conceptual design for such a detector based on the LNG technology.

The megaton Water Cerenkov detector represents the conservative approach, while the “100 kton liquid Argon” is certainly a very challenging design. Given the foreseeable timescale of more than a decade for the next generation of massive underground detectors, it is our conviction that a certain level of risk and challenge represents the most attractive way towards potential progress in the field.

## Acknowledgments

We thank I. Gil-Botella, A. Ereditato, A. Meregaglia and M. Messina for their help in the preparation of this presentation. This work was supported by ETH/Zurich and the Swiss National Research Foundation.



## References

- [1] H.Georgi and S.L.Glashow, Phys. Rev. Lett. **32** (1974) 438.
- [2] U.Amaldi, W. de Boer H.Füsternau, Phys. Lett. **B260** (1991) 447
- [3] G. Battistoni *et al.*, Nucl. Instrum. Meth. A **245**, 277 (1986).
- [4] G. Battistoni *et al.*, Phys. Lett. B **133** (1983) 454.
- [5] C. Berger *et al.* [FREJUS Collaboration], Nucl. Instrum. Meth. A **262** (1987) 463.
- [6] C. Berger *et al.* [Frejus Collaboration], Phys. Lett. B **269**, 227 (1991).
- [7] J. L. Thron, Nucl. Instrum. Meth. A **283** (1989) 642.
- [8] Goodman, M. C. (Soudan 2 Collaboration) in 26th International Cosmic Ray Conference (ICRC 99), Salt Lake City, UT, 17-25 Aug 1999.
- [9] M. Koshiba, “Kamioka Nucleon Decay Experiment: Kamiokande Collaboration,” Lecture given at SLAC Summer Institute, July 1988.
- [10] R. Becker-Szendy *et al.*, Nucl. Instrum. Meth. A **324**, 363 (1993).
- [11] Y. Fukuda *et al.*, Nucl. Instrum. Meth. A **501**, 418 (2003).
- [12] M. Shiozawa, “Neutrino Super Beam, Detectors and Proton Decay”, Joint BNL/UCLA - APS workshop, March 2004, Brookhaven National Laboratory.
- [13] C. Rubbia, “The Liquid Argon Time projection Chamber: a new concept for Neutrino Detector”, CERN-EP/77-08, (1977).
- [14] E. Aprile, K. L. Giboni and C. Rubbia, “A Study Of Ionization Electrons Drifting Large Distances In Liquid And Solid Argon,” Nucl. Instrum. Meth. A **241**, 62 (1985).
- [15] P. Benetti *et al.* [ICARUS Collaboration], “A 3 Ton Liquid Argon Time Projection Chamber”, Nucl. Instrum. Meth. A **332**, (1993) 395.
- [16] P. Cennini *et al.*, [ICARUS Collaboration], “Performance Of A 3 Ton Liquid Argon Time Projection Chamber”, Nucl. Instrum. Meth. A **345**, (1994) 230.
- [17] F. Arneodo *et al.* [ICARUS Collaboration], “The ICARUS 50 l LAr TPC in the CERN neutrino beam”, arXiv:hep-ex/9812006.
- [18] S. Amerio *et al.* [ICARUS Collaboration], “Design, construction and tests of the ICARUS T600 detector, accepted for publication in Nucl. Instrum. Meth. A. and references therein.
- [19] S. Amoruso *et al.* [ICARUS Collaboration], “Measurement of the muon decay spectrum with the ICARUS liquid Argon TPC,” arXiv:hep-ex/0311040. The European Physical Journal C, Eur. Phys. J. C **33**, 233-241 (2004).
- [20] S. Amoruso *et al.* [ICARUS Collaboration], “Study of electron recombination in liquid Argon with the ICARUS TPC,” Accepted by Nucl. Instrum. Meth. A. In press.

- [21] M. Antonello *et al.* [ICARUS Collaboration], “Detection of Cerenkov light emission in liquid Argon,” Nucl. Instrum. Meth. A516 (2004) 348-363.
- [22] S. Amoruso *et al.* [ICARUS Collaboration], “Analysis of the liquid Argon purity in the ICARUS T600 TPC,” Nucl. Instrum. Meth. A516 (2004) 68-79.
- [23] F. Arneodo *et al.* [ICARUS Collaboration], “Observation of long ionizing tracks with the ICARUS T600 first half-module,” Nucl. Instrum. Meth. A 508, 287 (2003).
- [24] A. Rubbia, “Experiments for CP-violation: A giant liquid Argon scintillation, Cerenkov and charge imaging experiment?,” arXiv:hep-ph/0402110. To appear in *Proceedings of the II International Workshop on Neutrino Oscillations in Venice, December 2003, Italy.*
- [25] A. Rubbia, “Neutrino factories: Detector concepts for studies of CP and T violation effects in neutrino oscillations,” arXiv:hep-ph/0106088. Appeared in *Proceedings of the 9th International Symposium on Neutrino Telescopes, Venice, Italy, Mar 2001.*
- [26] Technodyne International Limited, Unit 16 Shakespeare Business Center Hathaway Close, Eastleigh, Hampshire, SO50 4SR, see <http://www.technodyne.co.uk>
- [27] F. Sauli, Nucl. Instrum. Meth. A 386 (1997) 531.
- [28] P. Jeanneret, J. Busto, J. L. Vuilleumier, A. Geiser, V. Zacek, H. Keppner and R. de Oliveira, Nucl. Instrum. Meth. A 500 (2003) 133.
- [29] R. Chandrasekharan, M. Messina, P. Otiougova, P. Picchi, F. Pietropaolo, A. Rubbia, in preparation.
- [30] B. Viren [Super-Kamiokande Collaboration], arXiv:hep-ex/9903029. Y. Hayato *et al.* [Super-Kamiokande Collaboration], Phys. Rev. Lett. **83** (1999) 1529 [arXiv:hep-ex/9904020]. M. Shiozawa *et al.* [Super-Kamiokande Collaboration], Phys. Rev. Lett. **81** (1998) 3319 [arXiv:hep-ex/9806014].
- [31] Y. Itow *et al.*, “The JHF-Kamioka neutrino project,” arXiv:hep-ex/0106019.
- [32] C. K. Jung, “Feasibility of a next generation underground water Cherenkov detector: UNO,” arXiv:hep-ex/0005046.
- [33] M. V. Diwan *et al.*, arXiv:hep-ex/0306053.
- [34] A. Ereditato and A. Rubbia, “Ideas for future liquid Argon detectors,” To appear in *Proceedings of the Third International Workshop on Neutrino-Nucleus Interactions in the Few GeV Region, NUINT04, March 2004, Gran Sasso, Italy.*
- [35] Z. Dai, A. Rubbia, P. Sala, “Simulation of Cosmic Muon Induced Background to Nucleon Decay Searches in a Giant 100 kton LAr TPC”, in preparation.